Int. J. Electrochem. Sci., 14 **(2019)** 11541 – 11548, doi: 10.20964/2019.12.72

International Journal of
ELECTROCHEMICAL
SCIENCE
www.electrochemsci.org

Short Communication

Facile Synthesis of Cobalt Phosphate Hydrate Nanosheets with Enhanced Nonenzymatic Glucose Sensing

Daojun Zhang[*], *Jiakai Li, Ruguang Li, Zimo Wang, Jingjing Wei, Xiaobei Zhang, Bei Jiang, Jingchao Zhang, Renchun Zhang*[*]

College of Chemistry and Chemical Engineering, Anyang Normal University, Anyang 455000, Henan, China
[*]E-mail: zhangdj0410@sohu.com, rczhang@aynu.edu.cn

Received: 1 June 2019 / *Accepted:* 20 September 2019 / *Published:* 29 October 2019

In recent years, reports have shown that two-dimensional material's unique properties provide highly accessible surface areas and abundant active sites for contact with target analyser, electrolyte, and electron during catalytic processes. Herein, cobalt phosphate hydrate nanosheets were synthesised via a mild solvothermal method at 140 °C for 12 h, which were adopted into nanosheet modified glass carbon electrode displaying excellent electrocatalytic performance toward glucose detection in basic electrolyte. Electrochemical analysis showed that cobalt phosphate hydrate based non-enzymatic sensor possesses excellent efficiency and stability, low detection limit, and high anti-interference performance.

Keywords: Nanosheets; Electrochemical sensor; Non-enzymatic glucose detection

1. INTRODUCTION

Two-dimensional (2D) nanosheet materials have drawn considerable attention in recent years due to their unique properties, extending into multiple and diverse fields such as sensing, electrochemical energy storage, and optoelectronic devices [1,2]. Transition metal phosphates high electrochemical activities have evoked their use as supercapacitors, electrocatalytic splitting water, electrochemical sensors, and so on [3-5]. It has been extensively reported that blood glucose concentration levels are related to diagnosis and management of diabetes mellitus and other medical issues [6,7]. Therefore, the ease and rapidness of monitoring blood glucose levels is of crucial importance. Over the past few years, electrochemical techniques have been exploited to detect glucose due to its unique merits [8,9]. Numerous nanomaterials exhibit electrocatalytic activity and have been exploited in the construction of electrode materials for nonenzymatic glucose detection [10]. 2D nanomaterials possess high specific surface areas providing reliable electrochemical sensing

performance, enhancing sensitivity and stability. To date, the modification of electrode material involves the utilisation of metal oxides, sulphides, and hydroxides, for the purpose of non-enzymatic electrochemical glucose sensors [11-17]. In this paper, we report the preparation of novel cobalt phosphate hydrate nanosheets via a facile solvothermal method, which were used in the modification of glassy carbon electrode (CPH-GCE). The prepared 2D nanosheet modified electrode displayed high stability and excellent electrocatalytic activity for nonenzymatic glucose detection in basic solution. CPH-GCE showed excellent performances with low detection limit, wide linear range, good stability and high selectivity.

2. EXPERIMENTAL

2.1 Preparation of cobalt phosphate hydrate nanosheets

Typical synthesis of cobalt phosphate hydrate nanosheets is as follows: oleic acid (3.25g), octadecylamine (0.75g), ethanol (4.0 mL), and H_2O (4.0 mL) were added to a Teflon-lined autoclave (25 mL) and stirred until a homogeneous mixture was obtained. $Co(Ac)_4 \cdot 4H_2O$ (0.1 mmol) and NaH_2PO_4 solution (0.25 mL, 1 M) were added to the solution, followed by vigorous stirring for 60 min. The Teflon-lined autoclave was sealed and heated at 140 °C for 12 h. The purple product was isolated via centrifugation and washed with ethanol/cyclohexane (v/v=4:1) three times.

2.2 Electrochemical measurements

All electrochemical characterisation was performed on an electrochemical workstation (CHI 760E) with a three-electrode system. The bare GC electrode (3 mm) was carefully polished with 1.0, 0.3, and 0.05 μm Al_2O_3 powder prior to modifications with the catalyst. To prepare catalytic ink, 1.0 mg of the as-synthesised cobalt phosphate hydrate nanosheets was added to ultrapure water (1.0 mL) with ultrasonic dispersion. Then, 5.0 μL of the nanosheet suspension was casted on the GC electrode, and air dried at room temperature generating cobalt phosphate hydrate nanosheets modified GC electrode (CPH-GCE).

3. RESULTS AND DISCUSSION

3.1 Characterisation of cobalt phosphate hydrate nanosheets

Typical SEM images of as-synthesised cobalt phosphate hydrate are shown in Fig. 1a and 1b. Rectangular nanosheets with mean length of ~750 nm, width of ~460 nm, and thickness of several nanometres were observed by TEM with transparency configuration (Fig. 1c-d). However, lattice fringes were not detected for cobalt phosphate nanosheets through HRTEM images, indicating the lack of crystallinity of the obtained nanosheets. XRD pattern of the obtained cobalt phosphate sample is

exhibited in Fig. 2a, all peaks were indexed well to the standard crystallographic card (JCPDS card no. 34-0844) of $Co_3(PO_4)_2 \cdot 4H_2O$, indicating that the sample is of pure phase.

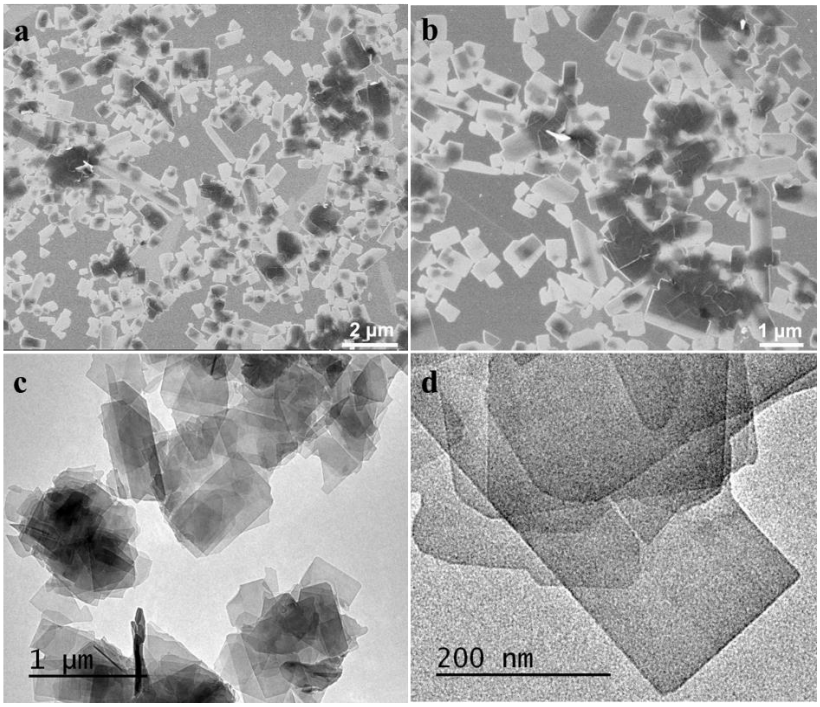

Figure 1. (a-b) SEM, (c-d) TEM images of cobalt phosphate hydrate nanosheets with low and high magnifition.

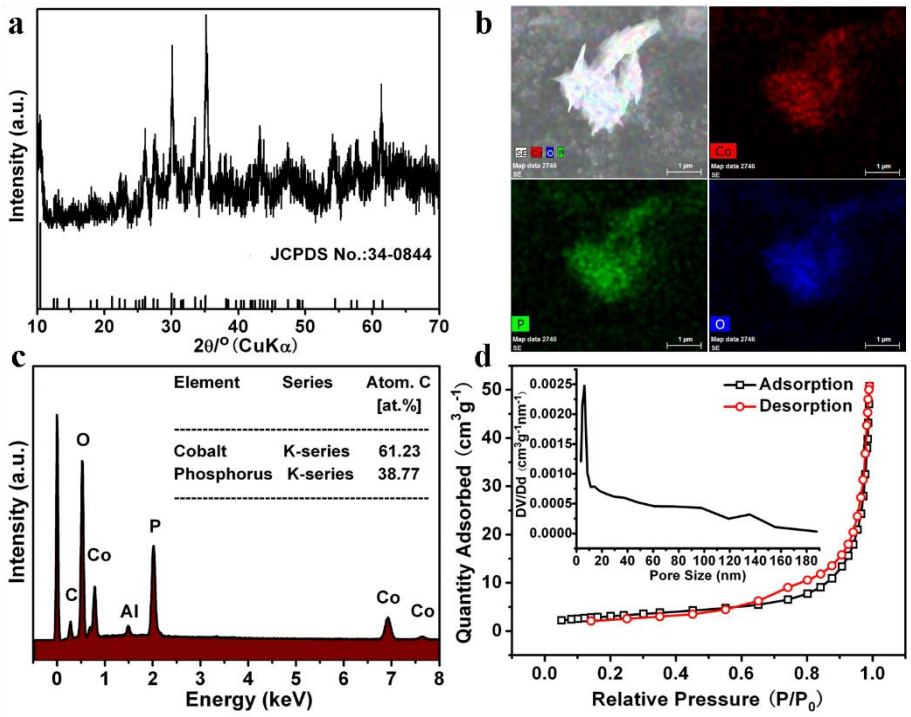

Figure 2. Characterization of cobalt phosphate hydrate nanosheets: (a) XRD pattern, (b) EDX mapping image, (c) EDX pattern, (d) Nitrogen adsorption-desorption isotherm and BJH pore size distribution plot (inset).

The element mapping of cobalt phosphate hydrate nanosheets displayed the homogenous distribution of Co, P and O (Fig. 2b), and, according to EDX characterization, Co/P ratio was ca. 3:2 (Fig. 2c) confirming cobalt phosphate hydrate composition. The BET surface area of cobalt phosphate hydrate sample was 11.16 m^2g^{-1}, using N_2 sorption isotherms (Fig. 2d). Therefore, the relatively high surface area and nanosheet structure provide more active sites for electrocatalytic reactions.

3.2 Nonenzymatic glucose sensor

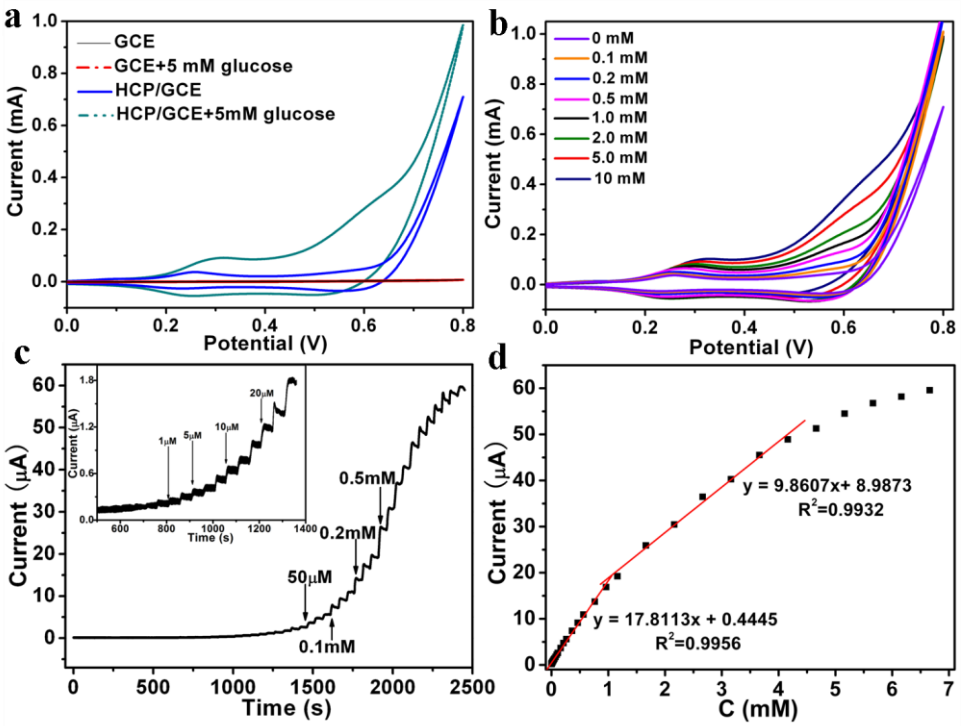

Figure 3. (a) CV curves of CPH/GCE in the absence (dotted line) and presence (solid line) of 5.0 mM glucose in 0.1 M NaOH. Scan rate: 50 mV/s. (b) CV curves of CPH/GCE adding of 0.1-10 mM glucose in 0.1 M NaOH. Scan rate: 100 mV/s. (c) Amperometric sensing of glucose by successive addition of glucose for CPH/GCE at 0.45 V in 0.1 M NaOH. Inset: Amperometic response at low concentration of glucose. (d) The corresponding calibration curves of the CPH/GCE for the glucose detection.

Electrochemical testing of cobalt phosphate hydrate sample was conducted to evaluate the catalytic performance for nonenzymatic glucose sensing. Fig. 3a shows the cyclic voltammograms (CVs) of CPH/GC and GC electrodes in the absence and presence of 5.0 mM glucose in 0.1 M NaOH solution. Compared with bare GCE, CPH/GC electrode exhibited a rapid increase in current density and two pairs of redox peaks at ~0.31/0.24 and 0.61/0.54 V, respectively, after the addition of 5.0 mM glucose. By increasing the glucose concentration a sharp increase in CPH/GC current density was also observed (Fig. 3b). Such a response was related to the greater availability of active sites on cobalt phosphate hydrate nanosheets for electrocatalytic reactions.

In alkaline solution, Co(II) on the surface of cobalt phosphate hydrate nanosheets modified

electrode was easily transformed to $Co(OH)_2$, which undergoes further oxidation generating CoOOH intermediate. The high valence Co(III) ions in CoOOH electrocatalyticly oxidised glucose to gluconolactone via electro-reduction of Co(III) to Co(II), which corresponds to the obvious redox peaks at ~0.31/0.24 V (Fig. 3a). In order to provide high current response and avoid oxidation of other small molecules, 0.45 V was chosen as the work potential for i-t experiments. Fig. 3c shows CPH/GC electrode typical amperometric response toward various glucose concentrations at 0.45 V in 0.1 M NaOH solution. Upon stirring the current response increased quickly after each addition of glucose. The calibration curve of glucose detection is shown in Fig. 3d, displaying a linear curve from 0.009 to 1.16 mM (R^2 = 0.9956) and 1.16 to 4.16 mM (R^2 = 0.9932). The as-prepared CPH/GC exhibited good response for nonenzymatic glucose sensing. As shown in Fig. 3c, the detection limit of CPH/GC electrode is 3.9 ìM (S/N=3), which is lower than Co nanobeads/rGO sensor (47.5 ìM) [11], CoOOH nanosheet arrays sensor (30.9 ìM) [22], Co_3O_4 nanocrystals sensor (50 ìM) [25], Pd–Au cluster (50 ìM) [28], and Co@Pt nanoparticles sensor (300ìM) [29]. There are two linear concentration ranges for the constructed sensor (Fig. 3d), in the low linear concentration range, the sensitivity is higher (251.92 μA $mM^{-1}cm^{-2}$), and in the high linear concentration range, the sensitivity is lower (139.47 μA $mM^{-1}cm^{-2}$). Both the sensitivity values of the constructed sensor CPH/GC electrode are higher than that of the reported Co nanobeads/rGO sensor (39.32 μA $mM^{-1}cm^{-2}$) [11], Co_3O_4 nanofibers modified electrode (36.25 ìA mM^{-1} cm^{-2}) [23] and Pd–Au cluster modified electrode (75.3 ìA mM^{-1} cm^{-2}) [28]. The phenomenon of two linear concentration ranges might be attributed to different oxidation kinetics at different glucose concentrations [31]. Glucose oxidation should be dominated by glucose adsorption at low glucose concentration, however, glucose activation became the rate-determining step at high concentration [31]. Many similar phenomena have been reported in the literature [32-35]. The performances include linear range, detection limit, and sensitivity of the cobalt phosphate hydrate modified electrode (CPH-GCE) were compared with other reported non-enzymatic electrochemical glucose sensors and summarized in Table 1. The CPH-GCE displays high sensitivity and low detection limit among the modified electrodes. The enhanced performance of the sensor may be ascribed to the unique cobalt phosphate structure with high surface area and large catalytic sites.

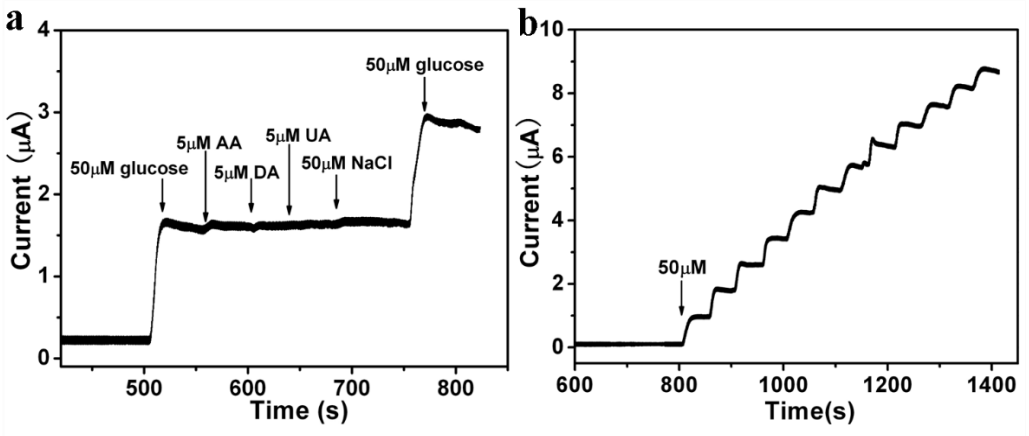

Figure 4. (a) The amperometric i–t curves of CPH/GCE to successive additions of 50 ìM glucose, 5.0 ìM AA, 5.0 ìM DA, 5 ìM UA, 50 ìM NaCl, and 50 ìM glucose in 0.1 M NaOH at 0.45 V. (b) Repeatable test of CPH/GCE by successive addition of 50 ìM glucose at the same condition.

The selectivity of the modified electrode was also a key factor that influenced performance. As shown in Fig. 4a, the successive addition of 50.0 ìM glucose, 5.0 ìM ascorbic acid (AA), 5.0 ìM uric acid (UA), 5.0 ìM dopamine (DA), 50.0 ìM NaCl, and 50.0 ìM glucose, had negligible responses for the above interfering species. The obtained results showed that CPH/GC electrode exhibited good selectivity toward glucose. The reproducibility and stability of the sensor was examined by measuring the amperometric response to successive addition of glucose. An RSD of 4.72% was attained after twelve successive determinations using the same electrode (Fig. 4b), highlighting the good reproducibility of the sensor. The experimental data obtained shows that prepared CPH/GC electrode is a candidate for nonenzymatic glucose sensing, possessing good reproducibility and stability.

Table 1. Comparison of the performance of CPH/GCE with other reported enzyme-free glucose sensors.

Electrode material	Potential (V)	Linear range/mM	Detection limit/μM	Sensitivity/μA $mM^{-1}cm^{-2}$	Ref.
ultrathin nickel−cobalt phosphate nanosheets	+0.55	0.002–4.47	0.4	302.99	4
Co nanobeads/rGO	+0.55	0.15–6.25	47.5	39.32	11
Cobalt oxide microspheres	+0.55	0.00083–8.61	0.46	669.78	20
Porous CoOOH nanosheet arrays	+0.52	0.003–1.109	1.37	526.8	21
CoOOH nanosheet arrays	+0.40	0.03–0.7	30.9	341.0	22
Co_3O_4 nanofibers	+0.59	Up to 2.04	0.97	36.25	23
Co_3O_4 porous film	+0.60	Up to 3.0	1	366.03	24
Co_3O_4 nanocrystals	+0.55	0.1–0.9	50	743.6	25
Octahedral Cu_2O	+0.60	0.3–4.1	128	241	26
Cobalt oxide nanoparticles/rGO	+0.45	0.04–4	1.44	1.21	27
Pd–Au cluster	–0.10	0.1–30	50	75.3	28
Co@Pt nanoparticles	–0.05	1–30	300	2.26	29
CuO_x–CoO_x/ graphene	+0.50	0.005–0.57	0.5	507	30
Cobalt phosphate hydrate nanosheets	+0.45	0.009–1.16 1.16–4.16	3.9	251.92 139.47	This Work

4. CONCLUSIONS

Cobalt phosphate hydrate nanosheets were synthesised and their morphology and composition characterized. The prepared cobalt phosphate hydrate nanosheets possessed abundant surface active sites and displayed excellent electrocatalytic activity for glucose oxidation. Furthermore, the oxidation potential of glucose decreased to only 0.45 V. Therefore, cobalt phosphate hydrate modified glass carbon electrode is a candidate as a nonenzymatic glucose sensor, demonstrating excellent performance and stability, low detection limit, and wide linear range. This research provides new insights into the development of highly efficient nonenzymatic glucose sensors.

ACKNOWLEDGMENTS
This work was supported by the National Science Foundation of China (No. 21603004, U1604119), and the Program for Innovative Research Team of Science and Technology in the University of Henan Province (18IRTSTHN006).

References

1. Y. F. Sun, S. Gao, F. C. Lei, C. Xiao, Y. Xie, *Acc. Chem. Res*., 48 (2015) 3−12.
2. C. L. Tan, X. H. Cao, X.J. Wu, Q.Y. He, J. Yang, X. Zhang, J. Z. Chen, W. Zhao, S. K. Han, G. H. Nam, M. Sindoro, H. Zhang, *Chem. Rev.*, 117 (2017) 6225−6331.
3. J. C. Zhang, Y. Yang, Z. C. Zhang, X. B. Xu, X. Wang, *J. Mater. Chem*. A, 2 (2014) 20182–20188.
4. Y. Shu, B. Li, J. Y. Chen, Q. Xu, H. Pang, X. Y. Hu, *ACS Appl. Mater. Interfaces*, 10 (2018) 2360−2367.
5. M. A. Z. G. Sial, H. F. Lin, X. Wang, *Nanoscale*, 10 (2018) 12975–12980.
6. G. F. Wang, X. P. He, L. L. Wang, A. X. Gu, Y. Huang, B. Fang, B. Y. Geng, X. J. Zhang, *Microchim Acta*, 180 (2013) 161–186.
7. C. Chen, Q. J. Xie, D.W. Yang, H.L. Xiao, Y.C. Fu, Y. M. Tan, S. Z. Yao, *RSC Adv*., 3 (2013) 4473–4491.
8. P. Si, Y. J. Huang, T. H. Wang, J. M. Ma, *RSC Adv*., 3 (2013) 3487–3502.
9. K. Dhara, D. R. Mahapatra, *Microchimica Acta*, 185 (2018) 49.
10. X. J. Liu, L. Long, W. X. Yang, L. L. Chen, J. B. Jia, *Sensors and Actuators* B, 266 (2018) 853–860.
11. Y. H. Song, C. T. Wei, J. He, X. Li, X. P. Lu, L. Wang, *Sensors and Actuators* B, 220 (2015) 1056–1063.
12. Y. H. Song, C. T. Wei, J. He, X. Li, X. P. Lu, L. Wang, *Sensors and Actuators* B, 220 (2015) 1056–1063.
13. G. L. Li, H. H. Huo, C. L. Xu, *J. Mater. Chem*. A, 3 (2015) 4922–4930.
14. 14.Y.Y. Su, B. B. Luo, J. Z. Zhang, *Anal. Chem*., 88 (2016) 1617−1624.
15. L.Wang, Y. L. Zheng, X. P. Lu, Z. Li, L. L. Sun, Y. H. Song, *Sensors and Actuators* B, 195 (2014) 1–7.
16. Y.W. Liu, X. Q. Cao, R. M. Kong, G. Du, A. M. Asiri, Q. Lu, and X. P. Sun, *J. Mater. Chem*. B, 5 (2017)1901–1904.
17. G. L. Li, H. H. Huo, C. L. Xu, *J. Mater. Chem*. A, 3 (2015) 4922–4930.
18. Y.Y. Su, B. B. Luo, J. Z. Zhang, *Anal. Chem*., 88 (2016) 1617−1624.
19. W. Huang, Y. Cao, Y. Chen, J. Peng, X. Y. Lai, J. C. Tu, *Appl. Surf. Sci*., 396 (2017) 804–811.
20. S.Q Ci, S. Mao,T. Z. Huang, Z. H. Wen, D. A. Steeber, J.H. Chen, *Electroanalysis*, 26 (2014) 1326–1334.
21. L. Zhang, C. L. Yang, G.Y. Zhao, J. S. Mu, Y. Wang, *Sensors and Actuators B*, 210 (2015) 190–196.

22. K. K. Lee, P. Y. Loh, C. H. Sow, W. S. Chin, *Electrochem.Commun.*, 20 (2012)128–132.
23. Y. Ding, Y. Wang, L. Su, M. Bellagambaa, H. Zhang, Y. Lei, *Biosens. Bioelectron.*, 26 (2010) 542–548
24. S. S. Fan, M.G. Zhao, L.J. Ding, J. J. Liang, J. Chen, Y.C. Li, S.G. Chen, *J. Electroanal. Chem.*, 775 (2016) 52–57.
25. M. Li, C. Han, Y. F. Zhang, X. J. Bo, L. P. Guo, *Anal. Chim. Acta*, 861(2015)25–35.
26. Y. C. Li, Y. M. Zhong, Y.Y. Zhang, W. Weng, S. X. Li, *Sensors and Actuators B*, 206 (2015) 735–743.
27. H. Heidari, E. Habibi, *Microchim Acta*, 183 (2016) 2259–2266.
28. J.P. Wang, Z. H. Wang, D.Y. Zhao, C. X. Xu, *Anal. Chim. Acta*, 832 (2014) 34–43.
29. H. Mei, W. Q. Wu, B. B. Yu, Y. B. Li, H. M. Wu, S. F. Wang, Q. H. Xia, *Microchim Acta*, 182 (2015)1869–1875.
30. S. J. Li, L.L. Hou, B. Q. Yuan, M. Z. Chang,Y. Ma, J. M. Du, *Microchim Acta*, 183 (2016) 1813–1821.
31. H. Y. Zhu, A. Sigdel, S. Zhang, D. Su, Z. Xi, Q. Li, S. H. Sun, *Angew. Chem. Int. Ed.*, 53 (2014) 12508–12512.
32. N. Karikalan, M. Velmurugan, S. M. Chen, C. Karuppiah, *ACS Appl. Mater. Interfaces*, 8 (2016) 22545−22553.
33. W. Huang, L.Y. Ge, Y. Chen, X.Y. Lai, J. Peng, J.C. Tu, Y. Cao, X. T. Li, *Sensors and Actuators B*, 248 (2017)169–177.
34. D. Xu, C. L. Zhu, X. Meng, Z. X. Chen, Y. Li, D. Zhang, S. M. Zhu, *Sensors and Actuators B*, 265 (2018) 435–442.
35. M. Ma, W. X. Zhu, D. Y. Zhao, Y. Y. Ma, N. Hu, Y. R. Suo, J. L. Wang, *Sensors and Actuators B*, 278 (2019) 110–116.

© 2019 The Authors. Published by ESG (www.electrochemsci.org). This article is an open access article distributed under the terms and conditions of the Creative Commons Attribution license (http://creativecommons.org/licenses/by/4.0/).